

## TEMPERATURE DEPENDENT ELECTRON AND HOLE CAPTURE CROSS SECTIONS OF THE MOLYBDENUM DEFECT IN SILICON

Bijaya B. Paudyal<sup>1</sup>, Keith R. McIntosh<sup>2</sup>, Daniel H. Macdonald<sup>3</sup> and Gianluca Coletti<sup>4</sup>

<sup>1,2</sup>Centre for Sustainable Energy Systems, Australian National University, Canberra, ACT 0200, Australia

<sup>1</sup>P: +612 6125 8299, F: +612 6125 0506, E: bijaya.paudyal@anu.edu.au

<sup>2</sup>P: +612 6125 8966, F: +612 6125 0506, E: krmcintosh@gmail.com

<sup>3</sup>College of Engineering and Computer Science, Australian National University, Canberra, ACT 0200, Australia

P: +61 2 612 52973, F: +612 6125 0506, E: daniel.macdonald@anu.edu.au

<sup>4</sup>ECN Solar Energy research Centre of Netherlands, NL-1755 LE Petten, The Netherlands

P: + 31 224 56 4382, F: +31 224 56 8214 , E: coletti@ecn.nl

**ABSTRACT:** The capture cross sections of both electrons  $\sigma_n$  and holes  $\sigma_p$  were determined for the defect formed by interstitial molybdenum in crystalline silicon over the temperature range  $-110$  to  $0$  °C. Carrier lifetime measurements were performed on molybdenum-contaminated silicon using a temperature controlled photoconductance instrument. Injection dependent lifetime spectroscopy was applied at each temperature to calculate  $\sigma_n$  and  $\sigma_p$ . This analysis involved a novel approach that independently determined the capture cross sections assuming a known defect density and thermal velocity. Both  $\sigma_n$  and  $\sigma_p$  were found to decrease with temperature in a fashion consistent with excitonic Auger capture.

**Keywords:** Capture cross section, Lifetime, Inductive coil

### 1 INTRODUCTION

Molybdenum (Mo) is a transition metal and a potential source of contamination in silicon devices [1]. Istratov *et al.* [2] measured a significant amount of Mo in commercially available multicrystalline silicon solar cells which can reduce the efficiency of solar cell by one third as reported by Davis *et al.* [3]. Mo remains in interstitial form within the lattice structure of silicon and creates an electrically active defect. Graff has summarised the published information about the electrical properties of Mo in silicon, mostly based on deep level transient spectroscopy (DLTS) [1]. The defect has a single defect energy level ( $E_t$ ), that is donorlike and exists at  $0.28 \pm 0.01$  eV above the valance band edge of silicon  $E_V$ .

Rohatgi *et al.* [4] applied DLTS coupled with dark and illuminated I-V measurements and concluded the defect energy to be  $E_t = E_V + 0.30$  eV. Hamaguchi *et al.* [5] applied DLTS and optical-DLTS to investigate the Mo-related defects in silicon and reported  $E_t = E_V + 0.31$  eV. Similarly Pettersson *et al.* [6] applied Junction Space Charge Techniques (JSCT) and located  $E_t = E_V + 0.298$  eV. Recently, Rein *et al.* [7] applied a combination of temperature and injection dependent lifetime spectroscopy to determine  $E_t$  and the ratio of capture cross sections ( $\sigma_n/\sigma_p$ ). Furthermore, he determined the T-dependent trend of the capture cross sections by measuring the lifetime at sufficiently low temperature.  $E_t$  determined by Rein *et al.* [7] was slightly higher than that determined by DLTS, however the value of  $\sigma_n/\sigma_p$  was about half. In this work we explicitly measure the temperature dependence of both  $\sigma_n$  and  $\sigma_p$ , from which we determine the temperature dependent trend of  $\sigma_n/\sigma_p$ .

This paper presents a novel and relatively simple technique for the determination of T-dependent expression for  $\sigma_n$  and  $\sigma_p$  using temperature and injection dependent lifetime spectroscopy (TIDLS) with a T-controlled photoconductance (PC) measurement instrument. Section two explains the carrier lifetime theory and its simplification in order to determine the temperature-dependent expression for  $\sigma_n$  and  $\sigma_p$ . This is followed by an

experimental section which presents the details of the measurement procedure, the instrument, and the preparation of Mo-contaminated samples for this work. In the results and discussion section, we present the temperature-dependent expressions for  $\sigma_n$  and  $\sigma_p$  and analyse their trends to determine the effective capture mechanism.

### 2 THEORY

The simplified version of the SRH lifetime [8, 9] for a single defect that does not behave like a trap (i.e.  $\Delta n = \Delta p$ ) can be written as [10]

$$\tau_{SRH} = \frac{\tau_{n0}(p_1 + p_0 + \Delta n) + \tau_{p0}(n_1 + n_0 + \Delta n)}{(n_0 + p_0 + \Delta n)}, \quad (1)$$

where  $\tau_{n0}$  and  $\tau_{p0}$  are the fundamental capture time constants for electrons and holes,  $n_1 = N_C \exp[(E_c - E_t)/k_B T]$  and  $p_1 = N_V \exp[(E_t - E_v)/k_B T]$ ,  $N_C$  and  $N_V$  are the effective densities of states at the conduction and the valance band edge,  $k_B$  is Boltzmann's constant,  $n_0$  and  $p_0$  are the electron and hole densities at thermal equilibrium, and  $\Delta n$  is the excess carrier density.

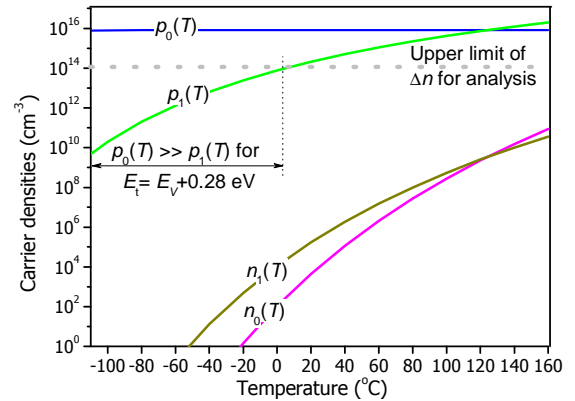


**Figure 1:** Carrier densities ( $n_1$ ,  $p_1$ ,  $n_0$  and  $p_0$ ) for a defect energy level ( $E_V + 0.28$  eV).

**Table 1.** Summary of the previous works

$\sigma_n$ (cm <sup>2</sup> )	$\sigma_p$ (cm <sup>2</sup> )	$\sigma_n / \sigma_p$ at 27 °C	$E_t$ (eV)	Ref and Technique
$4.21 \times 10^{-8} \times T^{-2.95}$	$7.60 \times 10^{-8} \times T^{-1.29}$	$11 \pm 2$	NA	This work, TIDLs
$1.6 \times 10^{-14}$ at 27 °C	$6.0 \times 10^{-16}$ at 27 °C	26.67	$E_v + 0.28$	[1], Average
NA	NA	NA	$E_v + 0.31$	[5], DLTS
NA	NA	NA	$E_v + 0.30$	[4], DLTS
$7.8 \times 10^{-15}$ at 27 °C	NA	13.0	$E_v + 0.317$	[7], TIDLs
NA	NA	NA	$E_v + 0.298$	[6], JSCT

For a p-type wafer,  $n_0$  can be neglected in comparison to  $p_0$  and when  $\Delta n$  is sufficiently less than  $p_0$ , the effective lifetime ( $\tau_{eff}$ ) can be expressed as,

$$\tau_{eff} = \frac{\tau_{no}(p_1 + p_0) + \tau_{po}(n_1 + n_0 + \Delta n)}{p_0}, \quad (2)$$

assuming that the overall recombination is dominated by SRH recombination.

For the temperature region where  $n_1(T) + n_0(T) \gg \Delta n$  is valid and  $p_1(T) \ll p_0(T)$  is valid, Equation (2) can be expressed as,

$$\tau_{eff} = \tau_{no} + \frac{\tau_{po}}{p_0} \times \Delta n. \quad (3)$$

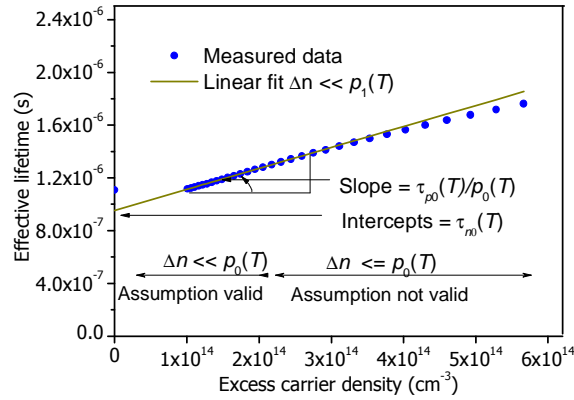


**Figure 2:** Measured lifetime data depicting linearity with the fitted model for  $\Delta n \ll p_0$  according to Equation (3)

The slope of a plot of  $\tau_{eff}$  against  $\Delta n$  therefore gives  $\tau_{po}/p_0$  and the intercept gives  $\tau_{no}$  as shown in Figure 2. Hence  $\sigma_n$  and  $\sigma_p$  can be calculated using the measured slope and the intercept of the linear plot  $\tau_{eff}$  against  $\Delta n$  for different temperatures as,

$$\sigma_p = \frac{1}{\tau_{po} v_{thp} N_T} = \frac{1}{Slope \times p_0 v_{thp} N_T}, \quad (4)$$

$$\sigma_n = \frac{1}{\tau_{po} v_{thn} N_T} = \frac{1}{Intercept \times v_{thn} N_T}, \quad (5)$$

where  $v_{thp}$  and  $v_{thn}$  are the thermal velocities of holes and electrons and  $N_T$  is the defect concentration.

### 3. EXPERIMENTS

A silicon ingot was grown at the Institut für Kristallzucht (IKZ) with the pedestal growth technique and boron-doped with a resistivity 1.8  $\Omega$  cm. The ingot

was intentionally contaminated by adding 2800 ppma of molybdenum in the silicon melt [11]. A Mo concentration of  $2 \times 10^{13} \text{ cm}^{-3}$  was determined by Neutron Activation Analysis (NAA) as described in detail elsewhere [11]. We assume that all of these Mo atoms are interstitial and active, and therefore  $N_T = 2 \times 10^{13} \text{ cm}^{-3}$ . The experiment was performed on a silicon sample sliced from the ingot. The wafer was subject to a phosphorus diffusion step with a sheet resistance of 50  $\Omega$  sq in an inline diffusion furnace. The emitter was then removed by a chemical polishing and a cleaning followed by a Plasma Enhanced-Chemical Vapour Deposition SiNx deposition optimised for surface passivation as described by Coletti *et al.* [12]. The average width of the sample was 285 microns. Lifetime measurements were performed on a temperature controlled inductive coil photoconductance based instrument, described in detail elsewhere [13].

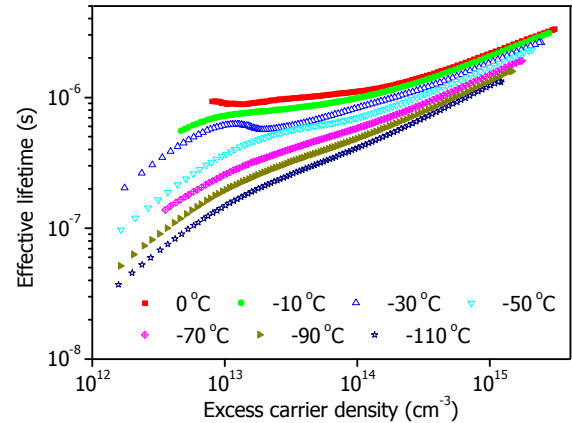


**Figure 3:** Injection dependent lifetime for temperatures - 110 to 0 °C in intervals of 10 °C.

The quasi-steady-state photoconductance (QSS PC) technique [14] was employed to determine the carrier lifetime at different temperatures. The carrier mobility model developed by Reggiani *et al.* [15] was applied for the subsequent analysis of the measured lifetime data. This mobility model only accounts the effect of temperature and dopant concentration and does not account the effect of  $\Delta n$ . The Reggiani model for carrier mobility was therefore modified by replacing the donor density  $N_D$  with  $N_D + \Delta n$  and the acceptor density  $N_A$  with  $N_A + \Delta n$ . This approximation was found to give a good agreement with the mobility model of Klaassen *et al.* [16, 17] at room temperature. Reggiani's carrier mobility model was preferred in this case because of its validity over a larger temperature range (-73 to 327 °C). The temperature across the wafers was found to vary by  $\pm 2\%$  during measurement and the uncertainty in the measured lifetime was  $\pm 6\%$  [13], which depends mostly upon the calibration of illumination intensity and inductive coil.  $\tau_{eff}$  was measured

as a function of  $\Delta n$  over a temperature range  $-110$  to  $0$  °C at intervals of  $10$  °C.

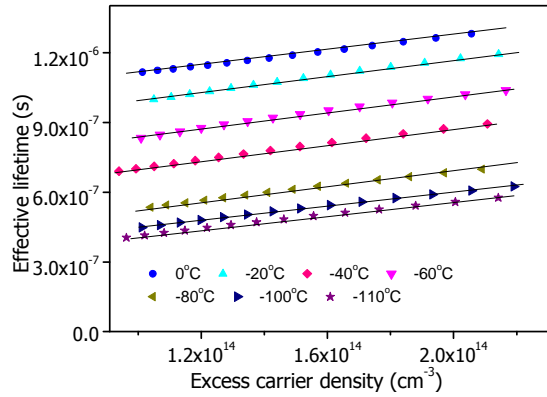


**Figure 4:** Lifetime plot of Mo-doped (1.8 Ohm cm) wafer for the selected injection range ( $1 \times 10^{14}$  -  $2. \times 10^{14}$   $\text{cm}^{-3}$ ).

#### 4. RESULTS AND DISCUSSION

$\tau_{\text{eff}}$  of the test wafer at low level injection ( $\Delta n < 2.2 \times 10^{14}$   $\text{cm}^{-3}$ ) was found to increase with temperature. The upper limit of temperature ( $T_{\text{max}}$ ) for which  $n_1(T) + n_0(T) \ll \Delta n$  is valid and  $p_1(T) \ll p_0(T)$  is determined to be  $0$  °C.  $n_1(T)$  and  $p_1(T)$  were calculated by using the reported values of  $E_t = 0.28$  eV [1], which gave most conservative  $T_{\text{max}}$ .  $n_0(T)$  was determined by using the doping density ( $N_A$ ) and the temperature dependent intrinsic carrier concentration,  $n_i(T)$  [18]. Freeze-out of the boron atoms in the wafer is taken into account at the low temperature ( $< 77$  °C) by adopting the T-dependent model of  $p_0(T)$  [19]. T-dependent models for the thermal velocities reported by Green *et al.* [18] is employed to calculate  $\sigma_n$  and  $\sigma_p$  using Equations 4 and 5.

The  $\Delta n$  range of  $1 \times 10^{14}$  to  $2 \times 10^{14}$   $\text{cm}^{-3}$ , which satisfies the above mentioned conditions for the Equations (2) and (3) is selected for the TIDLs analysis. The carrier densities ( $n_1$ ,  $p_1$ ,  $n_0$  and  $p_0$ ) and  $\Delta n$  for the analysis are depicted in Figure 1 for the defect energy level of  $E_V + 0.28$  eV in silicon. This graph shows  $n_1 + n_0 \ll 1 \times 10^{14}$   $\text{cm}^{-3}$  for the temperature less than  $160$  °C and  $p_1 \ll p_0$  for the temperature less than  $0$  °C. Table 2 depicts the temperature ranges for which the assumption  $(n_1 + n_0) \ll \Delta n$  and  $p_1 \ll p_0$  is valid for different reported values of  $E_t$ , where we require the negligible value to be no more than 1% of the significant value. Typical injection dependent lifetime plots over the  $\Delta n$  range chosen for analysis are depicted in Figure 3 for different temperatures.

Table 2: Temperature for which the assumptions  $(n_1 + n_0) < 0.01 \times \Delta n$  and  $p_1 < 0.01 \times p_0$  is valid for analysis.

$E_t$	$(n_1 + n_0) \ll \Delta n$	$p_1 \ll p_0$	Ref
$E_V + 0.28$ eV	$T \leq 160$ °C	$T \leq 0$ °C	[1]
$E_V + 0.30$ eV	$T \leq 158$ °C	$T \leq 10$ °C	[4]
$E_V + 0.317$ eV	$T \leq 155$ °C	$T \leq 18$ °C	[7]

The measured value of  $\sigma_p$  determined with Equation (4) is found to decrease with temperature over the temperature range  $-110$  to  $0$  °C. This indicates either Excitonic Auger Capture (EAC) [20] or cascade capture as

only two possible capture mechanisms [21]. The Multiphonon Emission Capture (MPE) [22] in which capture cross section increase with the temperature can be ruled out on this case. This temperature dependence of  $\sigma_p$  is best described by the EAC mechanism, with a temperature-independent pre-factor of  $\sigma_0 = 6.5 \pm 0.8 \times 10^{-14}$   $\text{cm}^2$  and the T-exponent of  $\alpha = -1.03 \pm 0.05$ , as shown in Equation (6). Figure 5 depicts the measured values of  $\sigma_p(T)$  with an EAC fit and previously published values. The calculated value of  $\sigma_p$  at  $27$  °C is  $1.86 \times 10^{-16}$  which is about 3 times less than the value reported by Graff [1] from DLTS data.

$$\sigma_p(T) = (6.5 \pm 0.8 \times 10^{-14}) T^{-(1.03 \pm 0.05)} \quad (6)$$

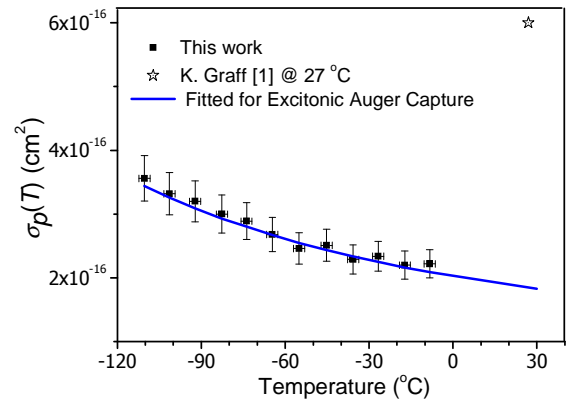


**Figure 5:** Hole capture cross section for Mo in silicon fitted for excitonic Auger capture mechanism.

Temperature-dependent values of  $\sigma_n$  are extracted by employing Equation (5) for the temperature range  $-100$  to  $0$  °C.  $\sigma_n$  is also found to decrease with temperature, and can be best described by an EAC mechanism. The EAC fit of the measured  $\sigma_n$  gives a temperature-independent pre-factor of  $\sigma_0 = 4.21 \pm 0.4 \times 10^{-8}$   $\text{cm}^2$  and the T-exponent of  $\alpha = -2.95 \pm 0.2$ . Measured values of  $\sigma_n$  fitted according to the EAC fit are extended to room temperature and compared with previously published values by Graff [1] and Rein [7] at room temperature as shown in Figure 6.

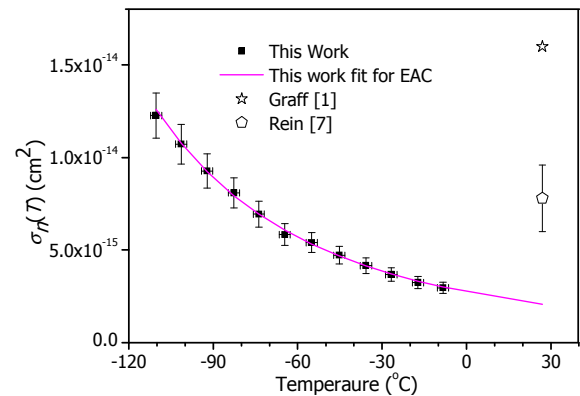


**Figure 6:** Electron capture cross section for Mo in silicon fitted with excitonic Auger capture mechanism and other previously published values at RT.

$$\sigma_n(T) = (4.21 \pm 0.4 \times 10^{-8}) T^{-(2.95 \pm 0.02)} \quad (7)$$

The capture cross section ratio ( $\sigma_n/\sigma_p$ ) was also found to be temperature dependent, even though both carriers are best described by the same capture mechanism (EAC). T-dependent  $\sigma_n/\sigma_p$  values are depicted in Figure 7. The extended value of  $\sigma_n/\sigma_p$  for room temperature agrees very well with the value reported by Rein *et al.* [7].

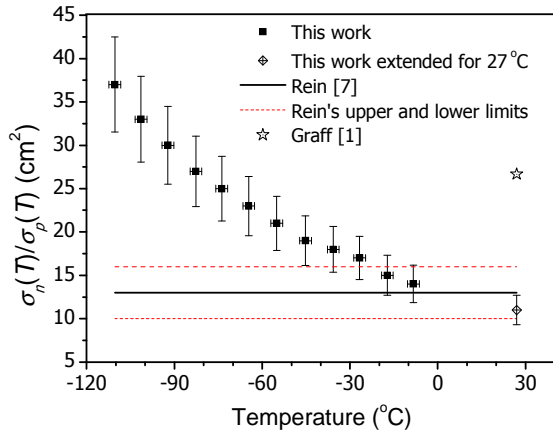


Figure 7: Capture cross section ratio of Mo defect in silicon at different temperatures.

The measured values of  $\sigma_n$  and  $\sigma_p$  for temperature range  $-110$  to  $0^\circ\text{C}$  depict a T-dependent trend which is used to calculate  $\sigma_n$  and  $\sigma_p$  at room temperature ( $27^\circ\text{C}$ ). Calculated values of  $\sigma_n$  and  $\sigma_p$  at room temperature were found lower than previously reported values [1, 7] as shown in Figure 5 and 6. A possible reason for this is the use of higher number of Mo defects ( $N_T$ ) for calculation of  $\sigma_n$  and  $\sigma_p$  than the exact number appeared in the test wafer as the active defect level. This may occur when all Mo atoms do not act as active defect [1]. This reason is further supported by the calculated value of  $\sigma_n / \sigma_p$  at room temperature which is not dependent upon  $N_T$  and gives a similar value to that reported by Rein [7]. Using a higher value of  $N_T$  for the calculation only lowers the T-independent pre-factors  $\sigma_0$  however it does not alter the T-dependent exponent ( $\alpha$ ), nor does it alter the conclusion that the capture mechanism is by EAC.

## 5. CONCLUSIONS

Temperature-dependent expressions for  $\sigma_n$  and  $\sigma_p$  of molybdenum in silicon were determined independently for the temperature range  $-110$  to  $0^\circ\text{C}$  using a temperature control photoconductance measurement device. The T-dependent trend of  $\sigma_n$  and  $\sigma_p$  best matched for the excitonic Auger capture mechanism, giving coefficients  $\sigma_0 = 4.21 \pm 0.4 \times 10^{-8}$ ,  $6.5 \pm 0.8 \times 10^{-14}$  and exponents  $\alpha = 2.95 \pm 0.2$  and  $1.03 \pm 0.05$ , where the uncertainty represents a 95 % confidence interval.

## ACKNOWLEDGEMENTS

This work was funded by an Australian Research Council Linkage Grant between the Australian National University, SierraTherm Production Furnaces, and SunPower Corporation. D. M. is supported by an Australian Research Council fellowship and G. C. is

supported by the "CrystalClear Integrated Project" (SES6-CT\_2003-502583) funded by European Commission.

## REFERENCES

- [1] K. Graff, *Metal impurities in silicon-device fabrication*: Springer-Verlag Berlin, 1995.
- [2] A. A. Istratov, T. Buonassisi, R. J. McDonald, A. R. Smith, R. Schindler, J. A. Rand, J. P. Kalejs, and E. R. Weber, *Journal of applied physics*, vol. 94, p. 6552, 2003.
- [3] J. R. Davis Jr, A. Rohatgi, R. H. Hopkins, P. D. Blais, P. Rai-Choudhury, J. R. McCormick, and H. C. Mollenkopf, *IEEE Transactions on Electron Devices*, vol. 27, pp. 677-687, 1980.
- [4] A. Rohatgi, R. H. Hopkins, J. R. Davis, R. B. Campbell, and H. C. Mollenkopf, *Solid-State Electronics*, vol. 23, pp. 1185-1190, 1980.
- [5] T. Hamaguchi and Y. Hayamizu, *Japanese Journal of Applied Physics*, vol. 30, pp. 1837-1839, 1991.
- [6] H. Pettersson, H. G. Grimmeiss, L. Tilly, K. Schmalz, K. Tittelbach, and H. Kerkow, *Semiconductor Science and Technology*, vol. 6, pp. 237-242, 1991.
- [7] S. Rein, *Lifetime spectroscopy: a method of defect characterization in silicon for photovoltaic applications*: Springer Verlag, 2005.
- [8] W. Shockley and W. T. Read, *Physical Review*, vol. 87, pp. 835-842, 1952.
- [9] R. N. Hall, *Physical Review*, vol. 87, pp. 387-387, 1952.
- [10] A. G. Aberle, "Crystalline silicon solar cells: advanced surface passivation and analysis," *The University of New South Wales*, 1999.
- [11] G. Coletti, L. J. Geerligs, P. Manshanden, C. Swanson, S. Riepe, W. Warta, J. Arumughan, and R. Kopecek, *Solid State Phenomena*, vol. 131, p. 15, 2008.
- [12] G. Coletti, R. Kvannd, V. D. Mihailitchi, L. J. Geerligs, L. Arnberg, and E. J. Øvrelid, *Journal of applied physics*, vol. 104, pp. 104913-104913, 2008.
- [13] B. B. Paudyal, K. R. McIntosh, D. H. Macdonald, B. S. Richards, and R. A. Sinton, *Progress in Photovoltaics: Research and Applications*, vol. 16, 2008.
- [14] R. A. Sinton and A. Cuevas, *Applied Physics Letters*, vol. 69, pp. 2510-2512, 1996.
- [15] S. Reggiani, M. Valdinoci, L. Colalongo, M. Rudan, G. Baccarani, A. D. Stricker, F. Illien, N. Felber, W. Fichtner, and L. Zullino, *IEEE Transactions on Electron Devices*, vol. 49, pp. 490-499, 2002.
- [16] D. B. M. Klaassen, *Solid-State Electronics*, vol. 35, pp. 953-959, 1992.
- [17] D. B. M. Klaassen, *Solid State Electron*, vol. 35, pp. 961-967, 1992.
- [18] M. A. Green, *Journal of applied physics*, vol. 67, p. 2944, 1990.
- [19] N. W. Ashcroft and N. D. Mermin, "Solid State Physics." 1976, *Saunders College, Philadelphia*, 1976.
- [20] A. Hangleiter, *Physical Review B*, vol. 37, pp. 2594-2604, 1988.
- [21] M. Lax, *Physical Review*, vol. 119, pp. 1502-1523, 1960.
- [22] C. H. Henry and D. V. Lang, *Physical Review B*, vol. 15, pp. 989-1016, 1977.